Proteome Partition Model with Three Sectors*

Jonathan (Shao-Kai) Huang†
Department of Physics, National Taiwan University

Wei-Hsiang Lin
Institute of Molecular Biology, Academia Sinica.
(Dated: December 15, 2025)

This study develops a mathematical model to predict proteome partitioning in bacterial cells, focusing on ribosomal content and its impact on growth rates. Using reaction networks, we model protein distribution across sectors like ribosomal, metabolic, and transport proteins. By applying Michaelis-Menten kinetics and Liebig's law of the minimum, we analyze how nutrient influx and protein allocation affect cell growth. Simulations identify optimal proteome partitions and steady-state solutions, revealing a strong correlation between growth rates and ribosomal protein content. The findings offer important insights into cellular resource allocation.

I. INTRODUCTION

A. Proteome Partition

Scott et al. (2010) proposed a three-sector proteome partition model to explain linear relationships arising in bacteria growth laws [1]. This model assumes Michaelis-Menten kinetics for its fluxes, so it is a scalable reaction network (SNR). The growth rate of SNRs exist, as shown by *Lin et al. (2020)* [2], so we can proceed to analyze this system of ODEs using various approximation and algebraic methods, with the goal of deriving the observed linear relationships without further empirical assumptions.

B. Scalable Reaction Networks

It is observed that during the exponential phase, all components of a bacteria cell grows exponentially with the same rate [3]. This is known as the **balanced growth condition**, and is essential in order to maintain exponential growth. Because of this, the number and biomass density of quantities remain nearly invariant during exponential growth. More recently, *flux-allocation models* in *Chure et al. (2023)* [4] showed that optimal allocation arises when translational flux and metabolic flux balance each other.

Michaelis-Menten kinetics can be derived from the assumption that substrate level is sufficiently high, and we will assume the system fluxes to be of the form (1).

$$\frac{\mathrm{d}[C]}{\mathrm{d}t} = \frac{V_{\mathrm{M}}[C]}{K_{\mathrm{M}} + [C]}. \tag{1}$$

C. Starvation and Excessive Nutrient

Nutrient availability profoundly shapes the physiology and proteome allocation of Escherichia coli. Under nutrient-limited conditions, such as carbon or nitrogen starvation, E. coli cells reduce growth rate to prioritize survival over proliferation. This includes upregulation of proteins involved in nutrient transport, while reducing the biosynthesis of ribosomes [1][5]. The stringent response, mediated by alarmone molecules like (p)ppGpp, plays a key role in reallocating proteomic resources decreasing ribosomal synthesis under starvation [6]. Conversely, when nutrients are abundant, E. coli cells exhibit acceleratted growth and allocate a larger fraction of the proteome to ribosomal proteins. Understanding how E. coli balances proteome partitioning across nutrient extremes is essential for elucidating fundamental principles of resource optimization.

II. THREE-SECTOR PARTITION MODEL

A. Model and Steady-State Solution

The model has 5 nodes and 5 fluxes, corresponding to the $n = 3$ case in figure 1. Each flux obeys Michaelis-Menten kinetics. The associated system of ODE obeyed by the *biomass fraction* is

$$\frac{\mathrm{d}Y_1}{\mathrm{d}t} = bY_3 - \frac{a_1 Y_1 Y_4}{k_1 + Y_1} - bY_3 Y_1, \tag{2}$$

$$\frac{\mathrm{d}Y_2}{\mathrm{d}t} = \frac{a_1 Y_1 Y_4}{k_1 + Y_1} - \frac{a_1 Y_2 Y_5}{k_2 + Y_2} - bY_3 Y_2, \tag{3}$$

$$\frac{\mathrm{d}Y_k}{\mathrm{d}t} = \theta_k \frac{a_1 Y_2 Y_5}{k_2 + Y_2} \ (k = 1, 2, 3). \tag{4}$$

It seems physically good that exchanging the two fluxes in the chain would not affect the growth rate. Below we will see that this is indeed the case.

---

* This research project is done under the guidance and supervision of Dr. Wei-Hsiang Lin.

† Also at Institute of Molecular Biology, Academia Sinica.; huang20041014@gmail.com

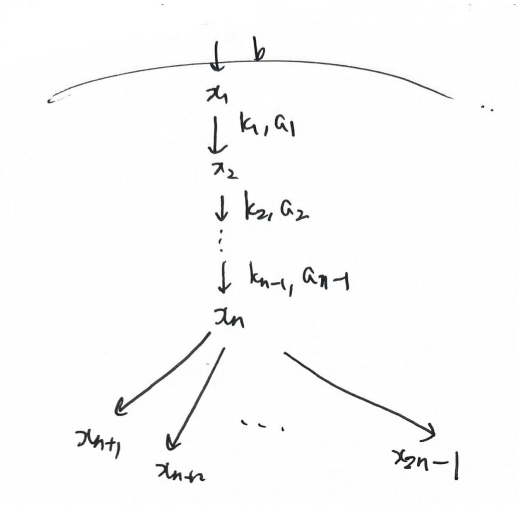

FIG. 1: Diagram of the nonlinear reaction network associated with the proteome partition model.

B. Approximate Theory

1. Starvation

During starvation, the nutrient level is reduced, so that $b/a_1, b/a_2 \ll 1$. We can expand the quantities in analytic form as a perturbative series in b (which turns out to be equivalent to an expansion in $b\theta_1$ or $b/a_1, b/a_2$) when nutrient level is low, for details see SI section 2B. Define the variables $A = \sqrt{\frac{k_1}{a_1}} + \sqrt{\frac{k_2}{a_2}}, B = \frac{k_1}{a_1} + \frac{k_2}{a_2}, C = \frac{a_1}{k_1} + \frac{a_2}{k_2}, D = \sqrt{\frac{k_1 k_2}{a_1 a_2}}, E = \frac{1}{a_1} + \frac{1}{a_2}$, which are all invariant under permutation of the indices. Then

$$\theta_1 = 1 - A\sqrt{b} - \frac{1}{2}A\left(2C - 3A^2 + 4D\right)b^{3/2}, \tag{5}$$

$$\theta_2 = \sqrt{\frac{k_1}{a_1}}\left[\sqrt{b} - \frac{1}{2}A^2 b^{3/2} - \left(AC - A^3 + 2AD\right)b^2\right], \tag{6}$$

$$\theta_3 = \sqrt{\frac{k_2}{a_2}}\left[\sqrt{b} - \frac{1}{2}A^2 b^{3/2} - \left(AC - A^3 + 2AD\right)b^2\right]. \tag{7}$$

Note that $\theta_1 = O(1)$, $\theta_2, \theta_3 = O(\sqrt{b})$. Using the above, let $R = Y_5^*$ be the ribosomal protein fraction and Small $= Y_1^* + Y_2^*$, Large $= Y_3^* + Y_4^* + Y_5^*$ be the fraction of small and large molecules, respectively. Then

$$R = \sqrt{\frac{k_2}{a_2}}\left[\sqrt{b} - Ab + \left(\frac{1}{2}A^2 + B + D - E\right)b^{3/2}\right], \tag{8}$$

$$\lambda = b - 2Ab^{3/2} + \left[2A^2 + B + D - E\right]b^2, \tag{9}$$

$$\text{Small} = A\sqrt{b} - \left(A^2 + B + D - E\right)b. \tag{10}$$

The small molecule fraction is invariant under exchange of indices, and since 1 is invariant, the large molecule fraction is also invariant.

The growth rate is parabolic in ribosomal content in the leading order.

$$\lambda = \frac{a_2}{k_2}R^2 - \left(\frac{a_2}{k_2}\right)^2(B + D - E)R^4 + O(R^5). \tag{11}$$

2. High Abundance of Nutrient

In the opposite limit, we can supply the cell with high levels of nutrient, such that $b/a_1, b/a_2 \gg 1$. This section will analyze the relevant dependencies.

Set $P = \theta_3/\theta_1 b, Q = \theta_2/\theta_1 b$. Numerical experiments with $a_1 = 23.8, a_2 = 1.42, k_1 = 0.1, k_2 = 0.003$ give the values $P \approx 0.350, Q \approx 0.007$, so $P \ll 1, Q \ll 1$ is justified.

Expanding to leading order in b^{-1} gives $\lambda(\theta) = \frac{Z}{b}\left(\frac{\theta_2\theta_3}{\theta_1}\right)$, $Z = a_1 a_2/[(1+k_1)k_2]$. Observe that the maximum of $\frac{\theta_2\theta_3}{\theta_1}$ occurs on the boundary, where $\theta_1 \to 0$, and consequently $\theta_2 = \theta_3 = \frac{1}{2}$ by the AM-GM inequality. The correct prediction should see $\theta_3 \to 1$, $\theta_2 \approx 0$, and $\theta_1 \to 0$, so an expansion to $O(b^{-2})$ is sought. Let

$$\alpha = \frac{k_2^2(1+k_1)^4 a_2}{(1+k_1+k_1k_2)^2 a_1^2 - k_2(1+k_1)^2 a_1 a_2 + (1+k_1)^4(1+k_2)a_2^2}, \tag{12a}$$

$$\beta = \frac{(1+k_1+k_1k_2)a_1 + (1+k_1)^2 a_2}{(1+k_1)^2 k_2}. \tag{12b}$$

Then

$$\theta_1 = \frac{1}{(2\alpha + \beta\alpha^2)b} + \frac{1}{(2\alpha+\beta\alpha^2)^2 b^2}, \tag{13a}$$

$$\theta_2 = \frac{\alpha}{2\alpha+\beta\alpha^2} - \frac{\alpha}{(2\alpha+\beta\alpha^2)^2 b} + \frac{\alpha}{(2\alpha+\beta\alpha^2)^3 b^2}, \tag{13b}$$

$$\theta_3 = \frac{\alpha+\beta\alpha^2}{2\alpha+\beta\alpha^2} - \frac{\alpha+\beta\alpha^2}{(2\alpha+\beta\alpha^2)^2 b} + \frac{\alpha+\beta\alpha^2}{(2\alpha+\beta\alpha^2)^3 b^2}. \tag{13c}$$

Note that $\theta_1 = O(b^{-1})$ and $\theta_2, \theta_3 = O(1)$. Although they seem to be of the same magnitude and the problem persists, the original problem is solved by noticing that

$$\frac{\alpha+\beta\alpha^2}{2\alpha+\beta\alpha^2} \gg \frac{\alpha}{2\alpha+\beta\alpha^2} \tag{14}$$

for α, β defined above and $a_1 \gg a_2, k_1 \gg k_2$.

The result for this limit has not yet been generalized to n sectors. Using the above result, the trajectories are found to be

$$Y_1 = 1 - Y_1^0 + O(b^{-2}), \tag{15a}$$

$$Y_2 = Y_2^0 + O(b^{-2}), \tag{15b}$$

$$Y_3 = O(b^{-1}), \tag{15c}$$

$$Y_4, Y_5 = Y_{4,5}^0 - O(b^{-1}). \tag{15d}$$

The growth rate goes like $bY_3 \sim \lambda^0 - O(b^{-1})$.

C. Lagrangian Analysis

Following the method proposed by Dr. Lin [7], we can analyze the system in the *Lagrangian* view.

The growth rate in the leading order is

$$\lambda = \lambda_0 - O(b^{-1}), \tag{16}$$

and the trajectories all behave asymptotically as $Y_j \sim$ const. $\mp\, O(b^{-2})$, where the leading constant term is a quantity close to 1 with $-$ sign for Y_1, while the leading term is a small quantity with $+$ for remaining fractions. This again matches the simulations. For trajectory equations, see SI.

III. GENERALIZED MODEL

The general system with n partitions is depicted in figure 1, and the associated system of ODEs is given in the SI. The analytic solution is best represented as a recursive formula.

$$Y_1 = \frac{1}{2}\left[\sqrt{\left(\frac{a_1\theta_2}{b\theta_1} + k_1 - 1\right)^2 + 4k_1} - \left(\frac{a_1\theta_2}{b\theta_1} + k_1 - 1\right)\right], \tag{17}$$

$$Y_j = \frac{1}{2}\left[\sqrt{\left(\frac{a_j\theta_{j+1}}{b\theta_1} + k_1 - \left(1 - \sum_{r=1}^{j-1} Y_r\right)\right)^2 + 4k_j} - \left(\frac{a_j\theta_{j+1}}{b\theta_1} + k_j - \left(1 - \sum_{r=1}^{j-1} Y_r\right)\right)\right] \quad (2 \le j \le n-1), \tag{18}$$

$$Y_j = \theta_{j-n+1}\left(\frac{a_{n-1}\theta_n}{b\theta_1}\right)\frac{Y_{n-1}}{k_{n-1} + Y_{n-1}} \quad (n \le j \le 2n-1). \tag{19}$$

By similar manipulations, the partition strengths are shown to be

$$\theta_2 : \theta_3 : \cdots : \theta_n = \sqrt{\frac{k_1}{a_1}} : \sqrt{\frac{k_2}{a_2}} : \cdots : \sqrt{\frac{k_{n-1}}{a_{n-1}}}. \tag{20}$$

$$\theta_1 = 1 - A_n\sqrt{b} + f(k_1, \ldots, k_n, a_1, \ldots, a_n)b + O(b^{3/2}), \tag{21}$$

where $A_n = \sum_{j=1}^{n-1}\sqrt{k_j/a_j}$ and f is a positive function on $(0,1)$ which is invariant under permutation of the index set $I = \{1, 2, \ldots, n\}$.

In the model with n partitions, and hence n metabolic steps leading up to node x_n, the dependence of growth rate λ on nutrient level b is still linear, the dependence of translational protein fraction $R \equiv Y^*_{2n-1}$ is still square root b, and hence the dependence of growth rate λ on R is still parabolic. Perhaps this could be interpreted as the fact that $\sqrt{}$ of the nutrient is being allocated to proteome partition section, while the other $\sqrt{}$ to the metabolic pathway itself.

IV. NUMERICAL RESULTS

A. Estimate of Parameters for Three-Sector Model

For realistic predictions and accurate qualitative analysis, we estimate the parameter values a_1, a_2, k_1, K_2 using *E. coli* as an example. In a single-cell organism, the number of per-cell protein is approximately 6×10^6.

Metabolic enzymes make up about 50% of the proteome, so $N_{\rm m} \approx 0.5 \times 6 \times 10^6 = 3 \times 10^6$. The average $k_{\rm cat}$ is 60 $\rm s^{-1}$, so $a_1 \approx k_{\rm cat}N_{\rm m}/N_{\rm total} \approx 30\ \rm s^{-1}$. The average half-saturation constant for metabolic enzymes is $K_{\rm M} \approx 100\,\mu$M, $k_2 \approx K_{\rm M}N_{\rm A}V/N_{\rm total} \approx 3.6 \times 6 \times 10^{-3}$.

Ribosomes take up about 20% of the proteome, and there are 52 r-proteins per ribosome, so $N_{\rm ribo} \approx 0.2 \times 6 \times 10^6/52 \approx 1.7 \times 10^4$ ribosomes. Elongation speed is $k_{\rm elon} = 16$ a.a./s, mean protein length is $L \approx 330$ a.a., volume of an E. coli cell is $V \approx 0.6\,\mu$m, so

$$\bar{a_2} \approx k_{\rm elon}N_{\rm ribo}/LN_{\rm total} \approx 1.4 \times 10^{-4}\ \rm s^{-1}. \tag{22}$$

The half-saturation constant for a.a.-tRNA is $K_{\rm M} \approx 3\,\mu$m, so $k_2 \approx K_{\rm M}N_{\rm A}V/N_{\rm total} \approx 1.8 \times 10^{-4}$.

Then $\bar{a}_1 \approx 5$ and $\bar{a}_2 \approx 1.42 \times 10^{-4}$. However, in the step $x_2 \to x_3$, we need about 2100 metabolites per protein (see SI). Account for stoichiometry and scale by 10^4 by changing time units, we have $a_1 \approx 23.8, \quad a_2 \approx 1.42$. Environmental nutrient quality is also scaled up, so b is on the magnitude of $1 \sim 10$. For the simulation, we run b over the range $0.01 \sim 100$.

B. Discussion of Results

The growth rate is the optimal value of the function $\bar{\lambda} = bY_3(\theta_1, \theta_2, \theta_3)$. Optimize over $\theta \in \Delta^2$, the result for numerical ODE solver, analytic solution agree very well (see SI).

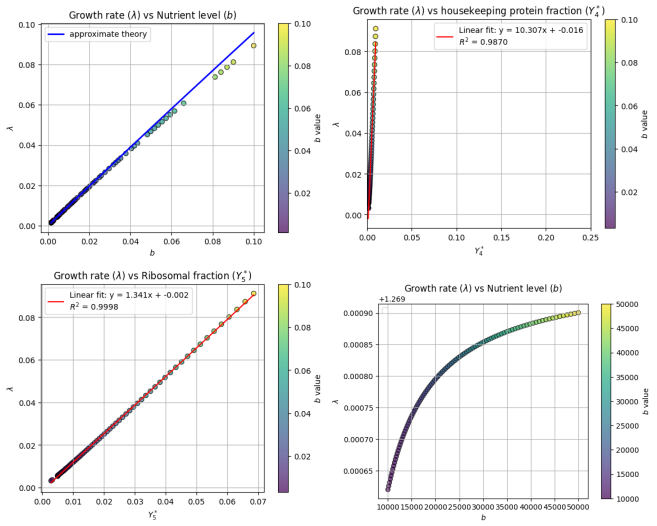

FIG. 2: (a) Growth rate is approximately linear in b with slope 1. Blue line is from theory. (b) The metabolic/housekeeping fraction is approximately constant. (c) Growth rate is parabolic in b near 0, and appears to be linear for higher b. (d) Growth rate with excessive nutrient.

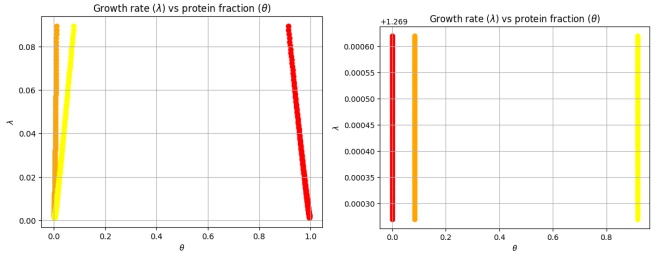

(a) (b)

FIG. 3: The proteome partition strength exhibits different strategies in different nutrient level. Red: θ_1. Orange: θ_2. Yellow: θ_3. See SI for a comparison against theory.

With the analytic solution, we can simulate λ and Y as functions of nutrient level b. Figure 2 shows trends under starvation.

The proteome partition strengths θ are plotted for varying b in the $b \to 0$ and the $b \to \infty$ limits. During starvation, more resources is allocated to transportation, while in excessive nutrient, the cell has reached its *optimal allocation strategy* and can no longer increase its efficiency: figures 3a and 3b.

In the high nutrient limit, figure 4 shows that the metabolic sector fraction is again nearly constant, as assumed in [1]. The analytic value of this constant fraction is topic of future discussion. Y_j vs b trajectories behave qualitatively differently during starvation and excessive nutrient. The trajectories are shown in SI, and can be

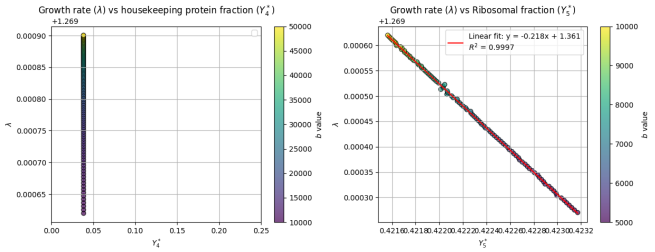

FIG. 4: (a) Metabolic sector is nearly constant. (b) Higher growth rate is correlated to lower ribosomal fraction, which is opposite to the starvation case.

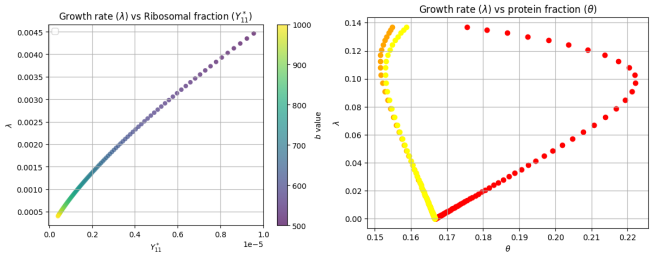

(a) (b)

FIG. 5: Abundant nutrient level. (a) Growth rate response to ribosomal protein fraction. Higher ribosomal fraction corresponds to higher growth rate, but higher nutrient level corresponds to lower growth rate. (b) Partition strength is non-monotonic.

summarized as

$$\text{low } b\text{: } Y_1 \nearrow\ Y_2 \nearrow\ Y_3 \searrow\ Y_4 \nearrow\ Y_5 \nearrow \tag{23}$$

$$\text{high } b\text{: } Y_1 \searrow\ Y_2 \searrow\ Y_3 \searrow\ Y_4 \searrow\ Y_5 \searrow \tag{24}$$

C. More Partitions and Relevant Results

With the increase of number of sectors, it becomes harder to keep track of each parameter. We choose a decreasing positive sequence of (a_j, k_j) to mimic the fact that metabolism is usually faster at the transporter, and becomes progressively slower down the reaction pathway.

Intermediate b value section that trajectories and growth rate may be non-monotonic. As nutrient level increases, the optimal allocation strategy changes non-monotonically. See figure 5.

Figure 6 shows growth rate trends in both limits. When nutrient level rises pass the low b limit, the convexity of the λ-b curve changes.

V. FUTURE WORK

- Analyze in the Lagrangian view.

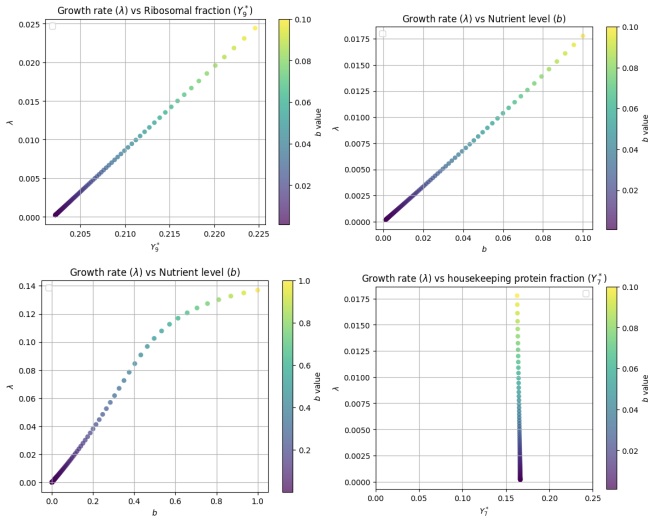

FIG. 6: (a) Starved growth rate versus ribosomal fraction for five sectors. (b) Starved growth rate versus nutrient level for six sectors. (c) When nutrient level rises, behavior of the λ-b curve with six partitions changes qualitatively. (d) One of the metabolic sectors with six sectors. The fraction is approximately constant.

- Study the distribution of protein fraction in the n metabolic sectors, given a positive monotonic sequence (a_j, k_j).
- The metabolic pathway involves a large diversity of biochemical reactions. Why can we coarse-grain them into two nodes only?
- Consider more general scalable flux functions such as polymer formation.
- Growth rate seems to be quadratic instead of linear in R during statrvation with Michaelis-Menten kinetics. Is this true experimentally, or is the approximation not accurate enough?
- Conduct analytical error analysis in the approximate theory.

[1] M. Scott, C. W. Gunderson, E. M. Mateescu, Z. Zhang, and T. Hwa, Interdependence of cell growth and gene expression: Origins and consequences, Science **330**, 1099 (2010), https://www.science.org/doi/pdf/10.1126/science.1192588.

[2] W.-H. Lin, E. Kussell, L.-S. Young, and C. Jacobs-Wagner, Origin of exponential growth in nonlinear reaction networks, Proceedings of the National Academy of Sciences **117**, 27795 (2020), https://www.pnas.org/doi/pdf/10.1073/pnas.2013061117.

[3] S. Cooper, *Bacterial Growth and Division: Biochemistry and Regulation of Prokaryotic and Eukaryotic Division Cycles*, 1st ed. (Academic Press, San Diego, CA, 1991) also available as an eBook (ISBN: 978-0080917474).

[4] G. Chure and J. Cremer, An optimal regulation of fluxes dictates microbial growth in and out of steady state, eLife **12**, e84878 (2023).

[5] S. Hui, J. M. Silverman, S. S. Chen, D. W. Erickson, M. Basan, J. Wang, T. Hwa, and J. R. Williamson, Quantitative proteomic analysis reveals a simple strategy of global resource allocation in bacteria, Molecular Systems Biology **11**, 784 (2015), https://www.embopress.org/doi/pdf/10.15252/msb.20145697.

[6] K. Potrykus and M. Cashel, (p)ppgpp: still magical?, Annual Review of Microbiology **62**, 35 (2008).

[7] W.-H. Lin, Biomass transfer on autocatalytic reaction network: a delay differential equation formulation (2025), arXiv:2210.09470 [q-bio.MN].